Pediatric Radiology (2019) 49:332–341
https://doi.org/10.1007/s00247-018-4319-1

ORIGINAL ARTICLE

Diagnostic performance of quantitative magnetic resonance imaging biomarkers for predicting portal hypertension in children and young adults with autoimmune liver disease

Jonathan R. Dillman[1,2,3] · Suraj D. Serai[1,4] · Andrew T. Trout[1,2,3] · Ruchi Singh[2,5] · Jean A. Tkach[1] · Amy E. Taylor[2,5] · Burns C. Blaxall[6] · Lin Fei[7] · Alexander G. Miethke[2,5]

Received: 23 August 2018 / Revised: 13 October 2018 / Accepted: 30 November 2018 / Published online: 3 January 2019

Abstract

Background Primary sclerosing cholangitis, autoimmune hepatitis and autoimmune sclerosing cholangitis are forms of chronic, progressive autoimmune liver disease (AILD) that can affect the pediatric population.

Objective To determine whether quantitative MRI- and laboratory-based biomarkers are associated with conventional imaging findings of portal hypertension (radiologic portal hypertension) in children and young adults with AILD.

Materials and methods Forty-four patients with AILD enrolled in an institutional registry underwent a research abdominal MRI examination at 1.5 tesla (T). Five quantitative MRI techniques were performed: liver MR elastography, spleen MR elastography, liver iron-corrected T1 mapping, liver T2 mapping, and liver diffusion-weighted imaging (DWI, quantified as apparent diffusion coefficients). Two anatomical sequences were used to document splenomegaly, varices and ascites. We calculated aspartate aminotransferase (AST)-to-platelet ratio index (APRI) and fibrosis-4 (FIB-4) scores — laboratory-based biomarkers of liver fibrosis. We used receiver operating characteristic (ROC) curve analyses to establish the diagnostic performance of quantitative MRI and laboratory biomarkers for indicating the presence of radiologic portal hypertension.

✉ Jonathan R. Dillman
jonathan.dillman@cchmc.org

[1] Department of Radiology,
Cincinnati Children's Hospital Medical Center,
3333 Burnet Ave., Cincinnati, OH 45229-3026, USA

[2] Center for Autoimmune Liver Disease (CALD),
Cincinnati Children's Hospital Medical Center,
Cincinnati, OH, USA

[3] Department of Radiology,
University of Cincinnati College of Medicine,
Cincinnati, OH, USA

[4] Department of Radiology,
Children's Hospital of Philadelphia,
Philadelphia, PA, USA

[5] Division of Gastroenterology, Hepatology, and Nutrition, Department of Pediatrics,
Cincinnati Children's Hospital Medical Center,
Cincinnati, OH, USA

[6] Heart Institute, Department of Pediatrics,
Cincinnati Children's Hospital Medical Center,
Cincinnati, OH, USA

[7] Division of Biostatistics and Epidemiology,
Cincinnati Children's Hospital Medical Center,
Cincinnati, OH, USA

Results Twenty-three (52%) patients were male; mean age was 15.2±4.0 years. Thirteen (30%) patients had radiologic portal hypertension. Liver and spleen stiffness demonstrated the greatest diagnostic performance for indicating the presence of portal hypertension (area-under-the-ROC-curve [AUROC]=0.98 and 0.96, respectively). The APRI and FIB-4 scores also demonstrated good diagnostic performance (AUROC=0.87 and 0.88, respectively).
Conclusion MRI-derived measures of liver and spleen stiffness as well as laboratory-based APRI and FIB-4 scores are highly associated with imaging findings of portal hypertension in children and young adults with AILD and thus might be useful for predicting portal hypertension impending onset and directing personalized patient management.

Keywords Autoimmune liver disease · Children · Liver · Magnetic resonance elastography · Magnetic resonance imaging · Multiparametric · Portal hypertension

Introduction

There are many causes of chronic liver disease in children and young adults, including autoimmune liver disease (AILD). AILD encompasses three separate clinical and histological entities, including primary sclerosing cholangitis (PSC), autoimmune hepatitis (AIH) and autoimmune sclerosing cholangitis (ASC, an overlapping condition with features of both sclerosing cholangitis and autoimmune hepatitis) [1, 2]. As with other chronic liver diseases, liver damage from chronic inflammation can result in myofibroblast activation, deposition of excess collagen and extracellular matrix, and the formation of fibrosis, or scar tissue [3]. Progressive liver fibrosis increases the resistance to blood flow through the liver and increases blood pressure in the portal venous system, ultimately causing portal hypertension, an important source of morbidity and mortality [4]. Portal hypertension can clinically and radiologically manifest as enlargement of the spleen (splenomegaly), development of portosystemic collateral vessels (varices), and ascites [5, 6].

There is increasing evidence that MRI can be used to detect, measure and follow chronic liver disease over time. Quantitative MRI techniques such as MR elastography, T1 mapping, T2 mapping and diffusion-weighted imaging (DWI) have been shown to correlate with the presence and degree of liver fibrosis to various degrees, although mainly in adult populations [7–11]. Although these techniques have been mostly employed to assess liver fibrosis burden, preliminary data suggest that MR elastography of the liver and spleen can be used to predict the risk or presence of portal hypertension and other quantitative MRI techniques might be able to do so, as well [12–14]. Quantitative MRI data could also likely be used to determine the rate of liver disease progression, predict the development of varices and ascites, and direct the need for interventions (e.g., endoscopic variceal screening).

Additionally, a small number of laboratory-based clinical biomarkers exist for detecting liver fibrosis and grading its severity. The aspartate aminotransferase (AST)-to-platelet ratio index, or APRI score, has been shown to detect significant liver fibrosis in adults with hepatitis C virus infection as well as numerous other chronic liver diseases, and in children with palliated biliary atresia [15–17]. Similarly, the fibrosis-4 (FIB-4) score has been demonstrated, again mostly in adults, to detect significant liver fibrosis in a variety of chronic liver diseases [18, 19]. The diagnostic performance of these clinical biomarkers has not been prospectively assessed for detecting and measuring liver fibrosis or predicting the presence of portal hypertension in a pediatric and young adult AILD cohort.

The primary purpose of our study was to determine whether multiple quantitative MRI biomarkers are associated with the presence of radiologic portal hypertension in children and young adults with AILD. As a secondary outcome, we sought to determine the relationships between laboratory-based APRI and FIB-4 scores and the presence of radiologic portal hypertension in the same patient population. If significant relationships were identified, longitudinal assessment of such biomarkers might be used in the clinic to predict impending portal hypertension, direct personalized patient management, and prognosticate patient outcomes. Finally, we sought to define the relationship between radiologic portal hypertension and important clinical outcomes such as endoscopic varices/gastrointestinal bleeding, clinically relevant ascites and liver transplant listing.

Materials and methods

Our institutional review board approved this cross-sectional study, which complied with the Health Insurance Portability and Accountability Act (HIPAA). Informed consent and informed assent were obtained, as appropriate. Perspectum Diagnostics (Oxford, UK) provided blinded image post-processing support for iron-corrected T1 (cT1) mapping at no cost through a formal research agreement. This study was partly funded by the Cincinnati Children's Hospital Medical Center's Center for Autoimmune Liver Disease and Center for Translational Fibrosis Research.

Forty-four children and young adults with AILD were enrolled in a prospective registry at the Center for Autoimmune Liver Disease at Cincinnati Children's Hospital Medical

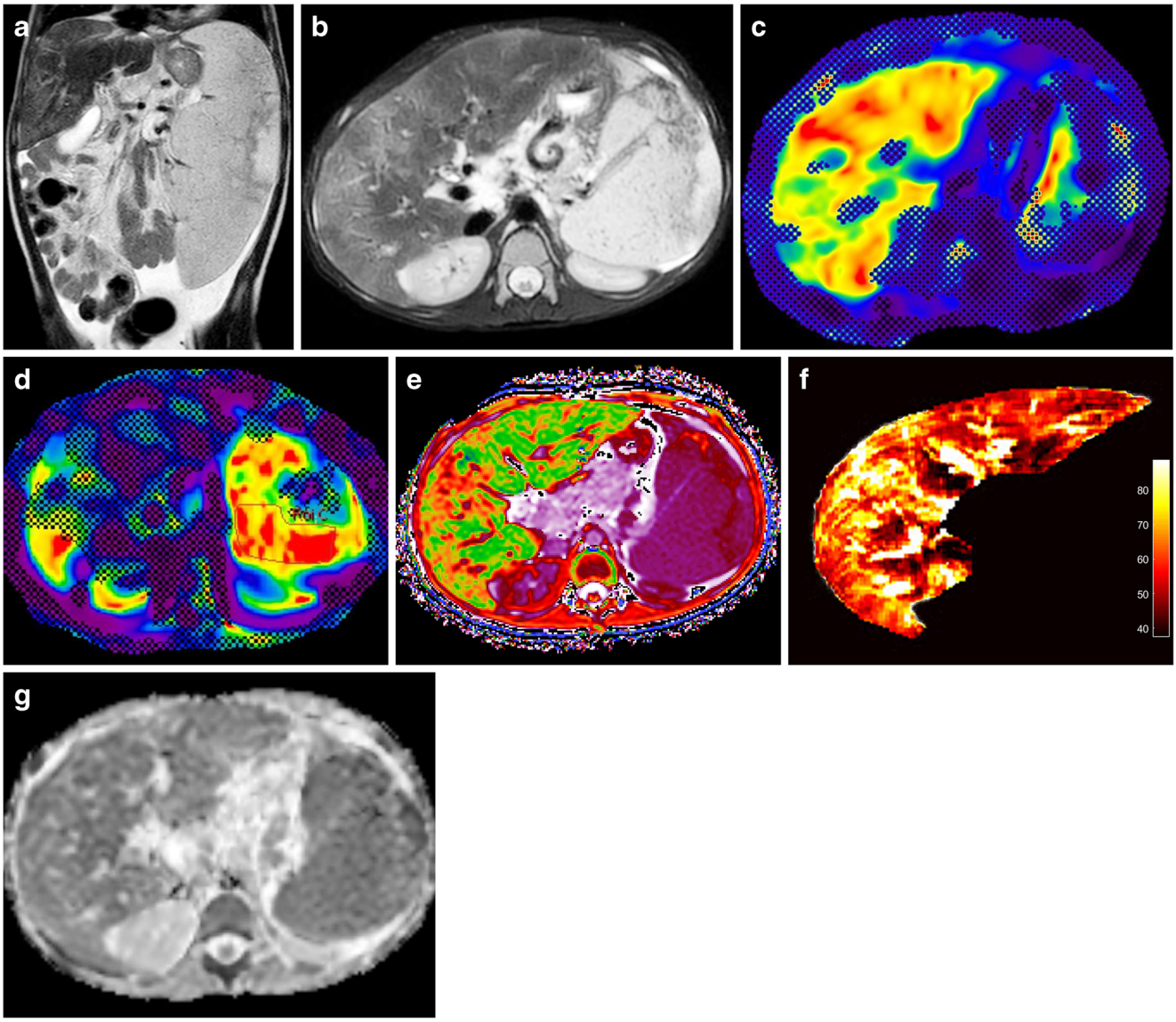

Fig. 1 Autoimmune liver disease in a 7-year-old boy. **a**, **b** Coronal single-shot fast spin-echo (**a**) and axial T2-weighted fast spin-echo fat-saturated (**b**) MR images show areas of geographic liver signal hyperintensity, marked splenomegaly (with an area of splenic infarction) and ascites. **c**, **d** MR elastography images of the liver (**c**) and spleen (**d**) show abnormally increased stiffness (4.8 kPa and 7.4 kPa, respectively). Note that the splenic region-of-interest was drawn to avoid the area of splenic infarction. **e**, **f** Iron-corrected T1 (cT1) (**e**) and T2 (**f**) maps show heterogeneous appearance of the liver with areas of focally increased T1 (mean=1,003.4 ms) and T2 (mean=66.0 ms) values, particularly in the right lobe. The T2 map shows mild motion artifacts. **g** Diffusion-weighted imaging apparent diffusion coefficient (ADC) map shows that the liver is diffusely hypointense, with lower than expected mean ADC value (0.93×10^{-3} mm^2/s)

Center. We approached children and young adults (ages 0 to 25 years) with a diagnosis of AILD (including PSC, AIH and ASC) and seen by a provider in the Division of Gastroenterology, Hepatology, and Nutrition about registry participation (www.clinicaltrials.gov; identifier number NCT03178630); registry enrollment is ongoing. The registry was started in fall 2016 and allows for the collection of pertinent demographic, clinical, laboratory, radiologic and histopathological data.

As a part of registry participation, participants underwent a multi-parametric research MRI examination at a field strength of 1.5 T (Ingenia; Philips Healthcare, Best, the Netherlands). Imaging parameters are listed in Appendix 1 [11, 20]. Two sets of anatomical images were obtained, including coronal single-shot fast spin-echo and axial T2-weighted fast spin-echo fat-suppressed imaging. Five axial sets of quantitative MRI images also were acquired, including:

1) Two-dimensional (2-D) gradient recalled echo (GRE) MR elastography of the liver (active driver frequency=60 Hz), with the passive driver placed over the right upper quadrant;

2) 2-D GRE MR elastography of the spleen (active driver frequency=60 Hz), with the passive driver placed over the left upper quadrant;
3) Iron-corrected T1 mapping of the liver (cT1) using a modified Look-Locker (MOLLI) pulse sequence approach [8];
4) T2 mapping of the liver using a multi-echo fast spin-echo approach; and
5) DWI of the liver, using five b values and quantified as apparent diffusion coefficients (ADC; Fig. 1).

For each quantitative MRI sequence, axial imaging was performed through the mid (widest portion) liver (or spleen) at multiple anatomical levels. Liver regions of interest (ROI) were drawn by an MRI clinical physicist (S.D.S., 10 years clinical MRI experience) on MR elastography elastograms, T2 maps and ADC maps, attempting to stay within the right hepatic lobe and segment IV of the left lobe and maximizing ROI size while avoiding visible blood vessels, bile ducts and areas of artifact. Spleen ROIs were drawn similarly to encompass as much parenchyma as possible. For each quantitative MRI biomarker and patient, we used the mean value for the four images (corresponding to the MR elastography levels) for analysis. For cT1, we used whole-liver ROIs on each of four axial slices, with the mean value provided by Perspectum Diagnostics.

Two radiologists (J.R.D., 9 years of post-fellowship experience, and A.T.T., 5 years of post-fellowship experience) reviewed coronal and axial T2-weighted anatomical images separately to document the presence of splenomegaly, varices and ascites. Reviewing radiologists knew patients had a diagnosis of AILD but were blinded to specific diagnoses as well as all clinical, laboratory and quantitative MRI data. Consensus review was used to manage any discrepancies. We defined splenomegaly as a craniocaudad splenic length that was more than two standard deviations above the mean length for participant age and gender [21]. For participants older than 17 years, we used the 17-year-old mean age and standard deviation. We defined varices as visible portosystemic collateral vessels seen in a variety of locations, such as the gastrohepatic ligament, adjacent to the esophagus and spleen, in the mesentery and omentum, and along the expected course of the umbilical vein. We defined ascites as any volume of free fluid in the peritoneal cavity, including adjacent to the liver or spleen.

Another author (A.E.T., 1 year of post-fellowship experience in pediatric gastroenterology) searched electronic medical records to document gender, age at the time of research MRI, clinical diagnosis (e.g., PSC vs. ASC vs. AIH), pertinent laboratory data, and whether a given patient had experienced any of the following at the time of MRI: endoscopic identification of varices/gastrointestinal bleeding, clinically relevant ascites (i.e., requiring paracentesis or diuretic therapy) and liver transplant listing.

We calculated the APRI and FIB-4 scores for each participant. We calculated the APRI score using the following formula: (AST participant level/AST upper limits of normal)/platelet count, where AST is in U/L and platelet count is 10^9/L. We calculated the FIB-4 score using the following formula: (age x AST participant level)/(platelet count x $\sqrt{}$ALT), where age is in years, AST is in U/L, platelet count is 10^9/L, and ALT is in U/L. Continuous data were summarized as means, standard deviations and ranges, while categorical data were summarized as counts and percentages.

We used receiver operating characteristic (ROC) curve analyses to establish the diagnostic performance of each quantitative MRI technique for indicating the presence of (1) splenomegaly (regardless of the presence or absence of other findings of portal hypertension) and (2) radiologic portal hypertension. A diagnosis of radiologic portal hypertension was based on the presence of any of the following: (1) varices alone; (2) splenomegaly and ascites; (3) splenomegaly and varices; or (4) splenomegaly, ascites and varices. We also used ROC curve analyses to assess the diagnostic performance of the laboratory-based APRI and FIB-4 scores for indicating splenomegaly and radiologic portal hypertension. Cut-off values for the various MRI and laboratory-based biomarkers were established based on the Younden J statistic in order to maximize both sensitivity and specificity. Techniques were compared using area-under-the-ROC-curve (AUROC) with 95% confidence intervals (CI).

We used the Fisher exact test to compare the frequency of important clinical outcomes/complications in participants without and with radiologic portal hypertension. A P-value <0.05 was considered statistically significant for inference testing. We performed statistical analyses using GraphPad Prism version 7 for Windows (GraphPad Software, La Jolla, CA) and R 3.4.0 (pROC package). Because our study was exploratory in nature based on an existing prospective, longitudinal institutional registry of pediatric and young adult AILD patients, no formal sample size analysis was performed prior to the data analyses described here.

Results

Our study included 44 registry participants with known AILD. Twenty-three (52%) participants were male. Mean participant age was 15.2±4.0 years (range 7.5–23.5 years). Twenty-three subjects had a clinical diagnosis of AIH, 13 had PSC and eight had ASC. See Table 1 for additional demographics.

Based on anatomical imaging, 22 (50%) participants had splenomegaly, while 13 (30%) had radiologic portal hypertension. Study population MRI- and laboratory-based biomarker

Table 1 Baseline demographics and laboratory data (*n*=44)

	n (%)		
Disease classification	AIH 23 (52%)	PSC 13 (30%)	ASC 8 (18%)
Gender (male)	23 (52%)		
Inflammatory bowel disease	16 (38%)		
	Mean	Standard deviation	Range
Age at MRI (years)	15.2	4.0	7.5–23.5
Time since diagnosis (years)	2.9	3.0	0–12.0
ALT (U/L)	92	130	17–638
AST (U/L)	61	78	12–407
Platelets ($\times 10^9$/L)	223	124	34–520

AIH autoimmune hepatitis, *ALT* alanine aminotransferase, *ASC* autoimmune sclerosing cholangitis, *AST* aspartate aminotransferase, *PSC* primary sclerosing cholangitis

means, standard deviations and ranges are presented in Table 2.

Biomarkers and splenomegaly

Of the five quantitative MRI techniques, liver stiffness demonstrated the best diagnostic performance for indicating the presence of splenomegaly (AUROC=0.87; Fig. 2), followed by spleen stiffness (AUROC=0.80). Using a liver stiffness cut-off value of greater than 2.8 kPa, MR elastography had a sensitivity of 86.4% and specificity of 77.3% for indicating the presence of splenomegaly.

Of the two laboratory-based clinical biomarkers, the APRI score demonstrated the best diagnostic performance for indicating the presence of splenomegaly, with an AUROC and associated confidence interval similar to that of liver MR elastography (AUROC=0.83). Using a cut-off value of >0.42, the APRI score had a sensitivity of 85.7% and specificity of 76.2% for indicating the presence of splenomegaly.

The diagnostic performance for all evaluated MRI and clinical biomarkers for indicating splenomegaly, including AUROCs, sensitivities and specificities, are presented in Table 3.

Biomarkers and radiologic portal hypertension

Of the five quantitative MRI techniques, liver and spleen stiffness demonstrated nearly identical diagnostic performance for indicating the presence of portal hypertension (AUROC=0.98 and 0.96, respectively; Fig. 3). Using a liver stiffness cut-off value of greater than 3.9 kPa, MR elastography had a sensitivity of 92.3% and specificity of 93.6% for indicating the presence of portal hypertension. Using a spleen stiffness cut-off value of greater than 7.3 kPa, MR elastography had a sensitivity of 90.9% and specificity of 93.3% for indicating the presence of portal hypertension.

The two laboratory-based clinical biomarkers, the APRI and FIB-4 scores, demonstrated very similar diagnostic performance for indicating the presence of portal hypertension (AUROC=0.87 and 0.88, respectively; Fig. 4). Using a cut-off value of greater than 0.66, the APRI score had a sensitivity of 91.7% and specificity of 80.0% for indicating the presence of portal hypertension. Using a cut-off value of greater than 0.76, the FIB-4 score had a sensitivity of 84.6% and specificity of 93.3% for indicating the presence of portal hypertension.

The diagnostic performance for all evaluated MRI and laboratory-based biomarkers for indicating the presence of portal hypertension, including AUROCs, sensitivities and specificities, is presented in Table 4.

Table 2 MRI and laboratory-based biomarker means, standard deviations and ranges in our population of children and young adults with autoimmune liver disease

	Mean	Standard deviation	Range
Liver stiffness (kPa) (*n*=44)	3.4	1.4	1.6–8.0
Spleen stiffness (kPa) (*n*=41)	6.7	2.4	3.8–13.9
Liver cT1 (ms) (*n*=42)	987.8	73.4	853.0–1,175.0
Liver T2 (ms) (*n*=44)	61.7	5.1	54.7–77.2
Liver ADC ($\times 10^{-3}$ mm^2/s) (*n*=44)	1.21	0.15	0.94–1.87
APRI score (*n*=42)	1.08	1.25	0.10–4.66
FIB-4 score (*n*=43)	0.73	0.83	0.08–3.45

ADC apparent diffusion coefficient, *APRI* aspartate aminotransferase (AST)-to-platelet ratio index, *cT1* iron-corrected T1, *FIB-4* fibrosis-4

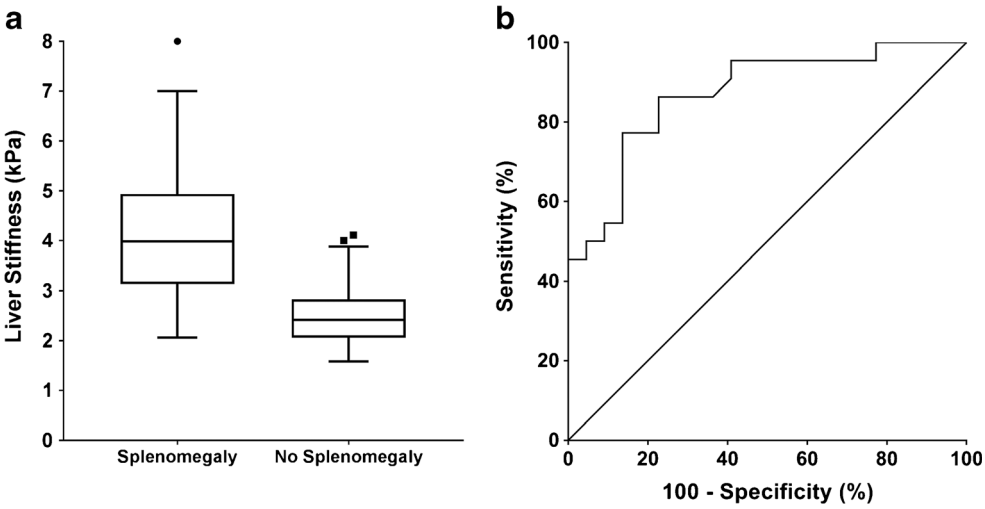

Fig. 2 Liver stiffness and splenomegaly. **a** Tukey box plot compares liver stiffness in registry participants with and without splenomegaly. **b** Receiver operating characteristic curve shows the diagnostic performance of liver stiffness for indicating the presence of splenomegaly (AUROC=0.87)

Association between radiologic portal hypertension and important clinical outcomes

Thirteen of 44 (30%) registry participants had radiologic findings of portal hypertension, including 8 with AIH, 3 with ASC and 2 with PSC. Ten of these 13 (77%) participants experienced one or more clinically important outcomes, compared to 0/31 (0%) participants without radiologic portal hypertension (P<0.0001; odds ratio >100 [>10.5–1,133]). Important clinical outcomes in these 10 individuals included endoscopic identification of varices/gastrointestinal tract bleeding (n=6), clinically relevant ascites (n=2) and liver transplant listing (n=7).

Discussion

A review of Table 2 shows that all of the quantitative MRI biomarkers assessed in our study are outside the normal range, on average, when compared to reported values in the literature for patients with no or mild liver disease. For example, for MR elastography of the liver, our population's mean stiffness was 3.4 kPa. In a paper by Xanthakos et al. [22], a stiffness of 2.71 kPa showed excellent diagnostic performance (AUROC=0.92) for detecting significant liver fibrosis in a pediatric population. A more recent study by Trout et al. [7] showed that a stiffness cut-off value of 2.49 kPa in a pediatric population without fatty liver disease was able to detect significant liver fibrosis with an AUROC of 0.82 (sensitivity=86%, specificity=71%). In a study of adults evaluating the diagnostic performance of cT1 in 79 unselected patients with paired MR imaging and biopsy data, and in 7 healthy volunteers, the volunteer values were on average 717±48 ms and the biopsied patients with no fibrosis were 750±42 ms [8]. This is in contradistinction to our patient population, which had a mean cT1 measurement of 987.8±73.4 ms.

Our data suggest that a single quantitative biomarker has satisfactory diagnostic performance for indicating the presence of splenomegaly, perhaps the earliest imaging and physical examination manifestation of portal hypertension. Liver stiffness measurements using MR elastography had an AUROC of 0.87 and was 86% sensitive and 77% specific, when maximizing diagnostic performance. When comparing other MRI biomarkers, AUROCs would not be clinically acceptable, with cT1, T2 and DWI ADC AUROCs being no

Table 3 Diagnostic performance of MRI and laboratory-based biomarkers for indicating presence of splenomegaly

	AUROC	95% CI	P-value[a]	Cut-off value	Sensitivity	Specificity
Liver stiffness (kPa)	0.87	0.77–0.98	<0.0001	>2.8	86.4%	77.3%
Spleen stiffness (kPa)	0.80	0.67–0.94	0.0009	>7.3	55.0%	95.2%
Liver cT1 (ms)	0.69	0.52–0.86	0.038	>949.5	81.0%	57.1%
Liver T2 (ms)	0.50	0.32–0.67	0.95	>61.8	50.0%	63.6%
Liver ADC ($\times 10^{-3}$ mm^2/s)	0.63	0.46–0.80	0.14	<1.14	45.5%	86.4%
APRI score	0.83	0.70–0.96	<0.0001	>0.42	85.7%	76.2%
FIB-4 score	0.79	0.64–0.93	0.0013	>0.44	63.6%	90.5%

ADC apparent diffusion coefficient, *APRI* aspartate aminotransferase (AST)-to-platelet ratio index, *AUROC* area under the receiver operating characteristic curve, *CI* confidence interval, *cT1* iron-corrected T1, *FIB-4* fibrosis-4

[a] A P-value <0.05 was considered statistically significant for inference testing

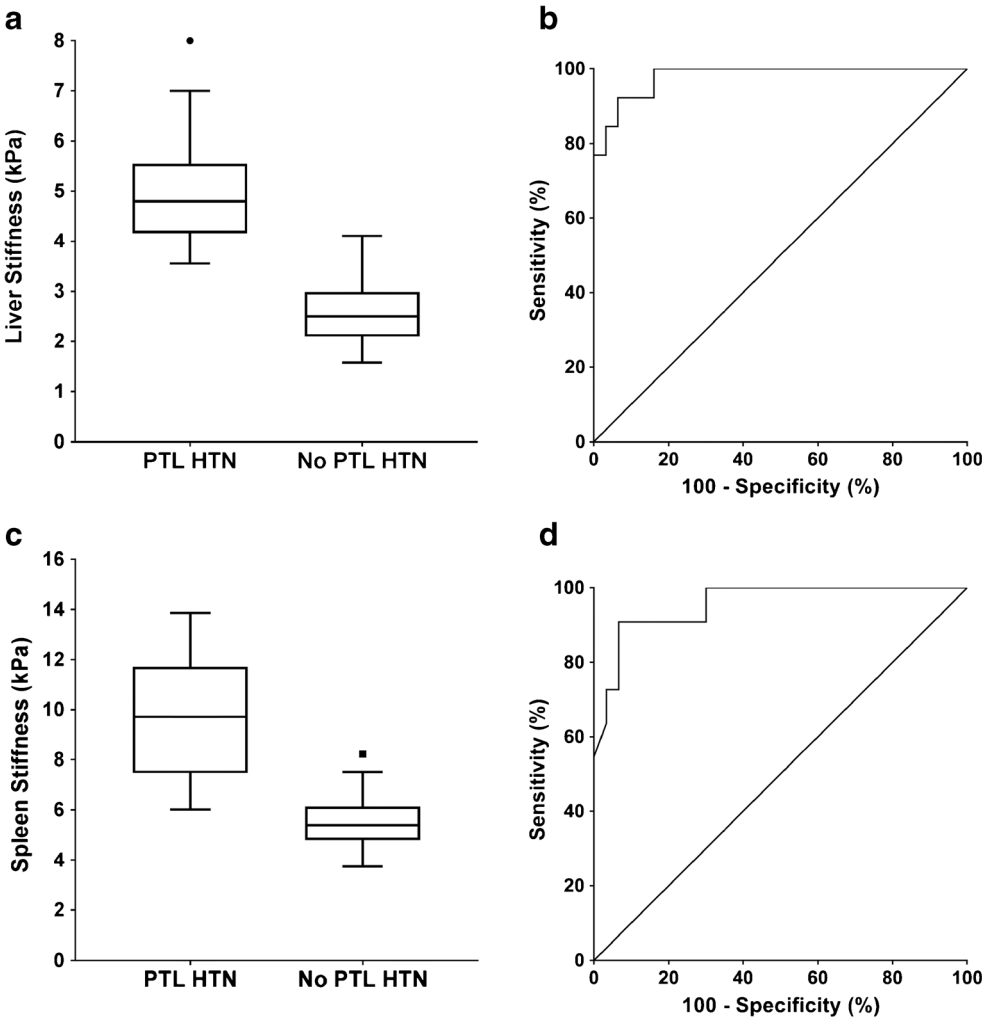

Fig. 3 Liver and spleen stiffness, and portal hypertension. **a** Tukey box plot compares liver stiffness in registry participants with and without portal hypertension. **b** Receiver operating characteristic curve shows the diagnostic performance of liver stiffness for indicating the presence of radiologic portal hypertension (AUROC=0.98). **c** Tukey box plot compares spleen stiffness in registry participants with and without portal hypertension. **d** Receiver operating characteristic curve shows the diagnostic performance of spleen stiffness for indicating the presence of radiologic portal hypertension (AUROC=0.96). *PTL HTN* portal hypertension

better or only slightly better than that what would be observed by chance when considering 95% confidence intervals. Surprisingly, the APRI score also showed respectable diagnostic performance for indicating the presence of splenomegaly with an AUROC of 0.83, having substantial overlap of the 95% confidence intervals for the AUROC values with liver stiffness. Further research comparing liver MRE and the APRI score for predicting impending splenomegaly is needed. This is in part because the APRI score is based on routine bloodwork and is likely to be a much cheaper biomarker,

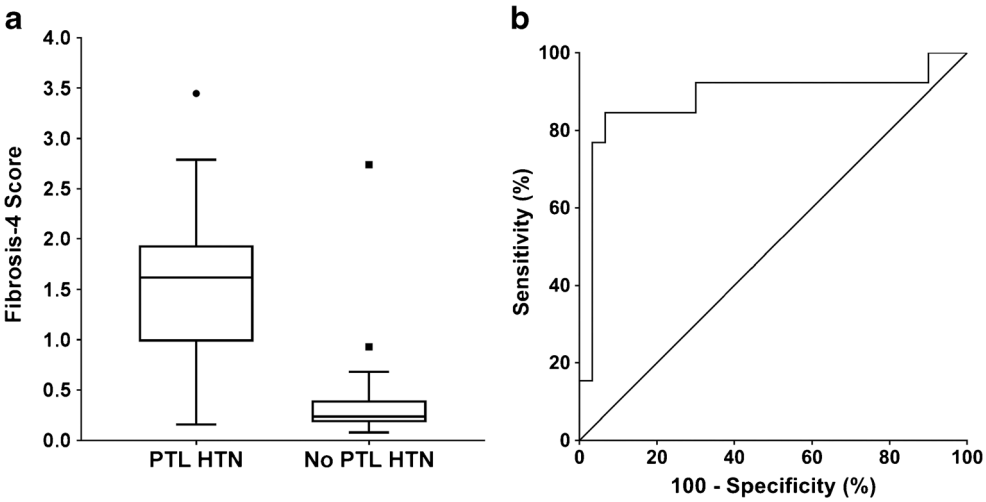

Fig. 4 Fibrosis-4 score performance and portal hypertension. **a** Tukey box plot compares fibrosis-4 (FIB-4) score in registry participants with and without radiologic portal hypertension. **b** Receiver operating characteristic curve shows the diagnostic performance of the FIB-4 score for indicating the presence of radiologic portal hypertension (AUROC=0.88). *PTL HTN* portal hypertension

Table 4 Diagnostic performance of MRI and laboratory-based biomarkers for indicating presence of radiologic portal hypertension

	AUROC	95% CI	*P*-value	Cut-off value	Sensitivity	Specificity
Liver stiffness (kPa)	0.98	0.95–1.00	<0.0001	>3.9	92.3%	93.6%
Spleen stiffness (kPa)	0.96	0.89–1.00	<0.0001	>7.3	90.9%	93.3%
Liver cT1 (ms)	0.86	0.75–0.97	0.0003	>1,001.3	84.6%	75.9%
Liver T2 (ms)	0.63	0.44–0.81	0.19	>60.0	76.9%	51.6%
Liver ADC ($\times 10^{-3}$ mm^2/s)	0.55	0.35–0.75	0.61	<1.18	53.8%	64.5%
APRI score	0.87	0.76–1.00	0.0002	>0.66	91.7%	80.0%
FIB-4 score	0.88	0.75–1.00	<0.0001	>0.76	84.6%	93.3%

ADC apparent diffusion coefficient, *APRI* aspartate aminotransferase (AST)-to-platelet ratio index, *AUROC* area under the receiver operating characteristic curve, *CI* confidence interval, *cT1* iron-corrected T1, *FIB-4* fibrosis-4

and the biomarker of choice, if shown to be equivalent or non-inferior to MR elastography liver stiffness.

Our data suggest that both liver and splenic stiffness acquired using MR elastography can detect radiologic portal hypertension with a high degree of diagnostic accuracy. AUROCs (0.98 and 0.96, respectively) were essentially identical for liver and spleen MR elastography with relatively similar 95% confidence intervals. These findings are similar to those in a prior study, by Ronot et al. [14], which found both liver and spleen stiffness to correlate with hepatic venous pressure gradients in adults with cirrhosis, some of whom had portal hypertension. Of note from their study, on multivariable analysis, spleen loss modulus (a quantitative measure that can be extracted from 3-D MR elastography that relates to a tissue's viscosity) had the highest predictive accuracy for both severe portal hypertension (AUROC=0.81) and high-risk varices (AUROC=0.93).

In our study, the AUROC for cT1 (0.86) for indicating radiologic portal hypertension was somewhat lower than those for liver and spleen MR elastography, although the 95% confidence intervals overlap. Liver T2 and DWI ADC values were poor indicators of portal hypertension. Interestingly, both the APRI and FIB-4 scores demonstrated essentially identical good diagnostic performance for indicating the presence of radiologic portal hypertension (AUROCs of 0.87 and 0.88, respectively). Again, more research is needed to determine whether there is a true difference in diagnostic performance between the imaging biomarkers (liver and spleen MR elastography), which utilize more resources, and the clinical laboratory-based biomarkers for indicating the presence of portal hypertension as well as predicting its impending onset.

Regarding the relationship between splenomegaly and radiologic portal hypertension, the onset of splenomegaly appears to occur at a lower liver stiffness, on average, than radiologic portal hypertension (2.8 kPa vs. 3.9 kPa, based on ROC curve analyses). Similarly, splenomegaly appears to be present, on average, at lower APRI and FIB-4 scores than radiologic portal hypertension (again, based on ROC curve analysis). This suggests that splenic enlargement might be an earlier manifestation of increasing portal pressure.

We also have demonstrated that the presence of radiologic portal hypertension is a risk factor for important clinical outcomes and morbidity in this specific patient population. In particular, radiologic portal hypertension, as defined in our study, seems to predict endoscopic identification of varices/gastrointestinal tract bleeding, clinically relevant ascites and liver transplant listing. Equally important, the absence of radiologic portal hypertension seems to indicate very low risk for these outcomes (0 such outcomes in 31 participants).

So, what do our results mean to children with chronic liver diseases? Given that there are significant positive associations between both MRI and laboratory biomarkers and splenomegaly (which may be an early feature of portal hypertension) and radiologic portal hypertension, we believe that these biomarkers and, in particular, their serial change over time might allow for the prediction of both portal hypertension and important associated clinical outcomes. Such outcomes might include rate of liver disease progression, both the short- and long-term risks of developing portal hypertension and its complications (e.g., variceal bleeding, intractable ascites), and need for intervention or changes in management such as endoscopic variceal screening. The cut-off values for liver and spleen stiffness — which are highly indicative of likely or impending portal hypertension — might help inform the selection of surrogate endpoints when designing clinical trials in the setting of pediatric-onset AILD. It is also conceivable that these biomarkers and their change over time might predict even more important outcomes such as time to liver transplant listing and time to actual transplant. It has not been established whether either the MRI- or laboratory-based biomarkers will ultimately be the better predictor, or whether there are additional predictive value and improved outcomes by combining multiple biomarkers (a so-called multiparametric approach).

Our study has limitations. First, it includes only 44 participants, 13 of whom had radiologic findings of portal hypertension. However our study is prospective and investigates a

rare group of diseases, yields several significant results, and provides promising pilot data that should serve as the basis for future validation investigations, including multi-institutional and longitudinal studies. Second, our primary outcome is radiologic portal hypertension. The most sensitive methods for detecting early portal hypertension are invasive catheter-based techniques that can provide measurements of pressure in the portal venous system. That said, our ultimate outcome is generalizable, easy to assess (is there splenomegaly, ascites or varices on cross-sectional imaging?), and clinically relevant. In fact, we have demonstrated that its presence is highly associated with important clinical outcomes, such as varices/gastrointestinal tract bleeding and liver transplant listing. Finally, while we have shown that numerous biomarkers are clearly associated with and can indicate the presence of splenomegaly and radiologic portal hypertension with satisfactory diagnostic performance, additional prospective studies employing longitudinal assessments are necessary to determine their predictive abilities and value in clinical practice.

Conclusion

Both quantitative MRI- and clinical laboratory-based biomarkers are associated the presence of splenomegaly and radiologic portal hypertension in pediatric and young adult patients with AILD. It is possible that MRI- or laboratory-based biomarkers, particularly when assessed longitudinally over time, can be used to predict impending portal hypertension and its associated risks, and thus can be used to more personally guide patient care and predict key outcomes. Additionally, we have demonstrated that the presence of radiologic portal hypertension is highly associated with important clinical outcomes in this patient population, while its absence is associated with likely very low risk for such outcomes, at least in the short term. Further research, including prospective longitudinal investigations, is needed to confirm our findings and to establish whether MRI-based biomarkers, laboratory-based biomarkers, or some combination of both provides the greatest predictive abilities and correlates best with the presence of (or impending) portal hypertension and other key clinical outcomes.

Acknowledgments This study was partially funded by: (1) a Cincinnati Children's Hospital Medical Center (CCHMC) Academic and Research Committee grant and (2) the CCHMC Center for Autoimmune Liver Disease. Iron-corrected T1 image processing was performed by Perspectum Diagnostics (Oxford, UK) at no cost through a research agreement.

Compliance with ethical standards

Conflicts of interest None

Appendix 1: Imaging acquisition

Liver magnetic resonance elastography

Liver MR elastography was performed using an active-passive driver system (Resoundant Inc., Rochester, MN) operated at 60 Hz and a two-dimensional gradient recalled echo pulse sequence. The passive driver was placed over the right upper quadrant. Four axial slices positioned to cover the widest portion of the liver were acquired in four consecutive breath-holds at end-expiration. Four time points (phases) of the vibration cycle were collected for each slice. Two axial spatial saturation slabs were placed parallel to the imaging volume (i.e. in the S/I direction) to suppress the signal from flowing blood. Additional acquisition parameters were as follows: repetition time/echo time (TR/TE)=50/20 ms, flip angle=20°, field of view (FOV)=380 mm, matrix=252×80, section thickness=10 mm, slice gap=1 mm, acceleration=2, receiver bandwidth=288 Hz/pixel, and number of averages=1. Elastograms with 95% confidence maps were generated on the scanner based on MRI displacement data (four phase and four magnitude images per slice) using a direct inversion algorithm based on the Helmholtz equation [11].

Spleen magnetic resonance elastography

Spleen MR elastography was performed in a manner identical to liver MR elastography with the following exceptions: the passive driver was placed over the left upper quadrant, the four axial slices were positioned to cover the widest portion of the spleen, the FOV was 450 mm, and the matrix was 300×96.

Liver iron-corrected T1 mapping (cT1)

Liver iron-corrected T1 mapping was performed using a breath-hold modified Look-Locker inversion recovery technique (MOLLI) [20]. The acquisition was electrocardiographically (ECG)-triggered, with a pulse oximeter providing the cardiac synchronization signal. The following MOLLI acquisition scheme was used: 5-s (s) acquisition, 3-s pause, 3-s acquisition — which resulted in an 11-s breath-hold during which images at multiple time points along the T1 recovery curve were collected at a given slice location. The exact number of time points collected was dependent on the duration of the participant's cardiac cycle. Four axial slices positioned to cover the widest portion of the liver were acquired in four consecutive 11-s breath-holds at end-expiration. Additional acquisition parameters were as follows: TR/TE=4.76/2.36 ms, flip angle=35°, FOV=440 mm, matrix=192×192, section thickness=8 mm, slice gap=7 mm, half Fourier=0.75, acceleration=2, receiver bandwidth=312 Hz/pixel, and number of averages=1. A multi-echo (n=8) gradient echo

(TE=2.37–18.96 ms) acquisition was also performed to provide an estimate of T2*, which was used for the T1 iron correction. Mean whole-liver cT1 measurements were provided by Perspectum Diagnostics (Oxford, UK), which was blinded to all other imaging and clinical data.

Liver T2 mapping

Liver T2 mapping was performed using a respiratory-triggered multi-echo fast spin-echo technique and a total of 20 echo times (TE), ranging 12–240 ms. Four axial slices positioned to cover the widest portion of the liver were acquired. Additional parameters were as follows: TR=3,000 ms, FOV=360, matrix=256×179, slice thickness=8 mm, slice gap=8 mm, acceleration=2.2, receiver bandwidth=150 Hz/pixel, and number of averages=1. T2 maps were generated offline using MATLAB (MathWorks, Natick, MA).

Liver diffusion-weighted imaging (DWI)

Liver DWI was performed using a respiratory-triggered fat-suppressed single-shot echoplanar imaging pulse sequence with 5 b values (0 mm^2/s, 100 mm^2/s, 200 mm^2/s, 500 mm^2/s and 800 mm^2/s). Twenty-seven axial slices positioned to cover the liver were acquired in three concatenations/packages. Four DWI images corresponding to the MR elastography anatomical levels were selected for analysis. Additional parameters were as follows: TR/TE=905/63.2 ms, FOV=400 mm, matrix=132×130, section thickness=6 mm, slice gap=0.6 mm, half Fourier=0.69, acceleration=2, receiver bandwidth=2,199 Hz/pixel, and number of averages=2. Apparent diffusion coefficient maps were generated by the scanner.

References

1. Deneau M, Jensen MK, Holmen J et al (2013) Primary sclerosing cholangitis, autoimmune hepatitis, and overlap in Utah children: epidemiology and natural history. Hepatology 58:1392–1400
2. Singh H, Balouch F, Noble C, Lewindon P (2018) Evolving practice and changing phenotype in pediatric autoimmune liver disease: outcomes from an Australian center. J Pediatr Gastroenterol Nutr 67:80–85
3. Sun M, Kisseleva T (2015) Reversibility of liver fibrosis. Clin Res Hepatol Gastroenterol 39:S60–S63
4. Deneau MR, El-Matary W, Valentino PL et al (2017) The natural history of primary sclerosing cholangitis in 781 children: a multicenter, international collaboration. Hepatology 66:518–527
5. Bloom S, Kemp W, Lubel J (2015) Portal hypertension: pathophysiology, diagnosis and management. Intern Med J 45:16–26
6. Brancatelli G, Federle MP, Ambrosini R et al (2007) Cirrhosis: CT and MR imaging evaluation. Eur J Radiol 61:57–69
7. Trout AT, Sheridan RM, Serai SD et al (2018) Diagnostic performance of MR elastography for liver fibrosis in children and young adults with a spectrum of liver diseases. Radiology 2018:172099
8. Banerjee R, Pavlides M, Tunnicliffe EM et al (2014) Multiparametric magnetic resonance for the non-invasive diagnosis of liver disease. J Hepatol 60:69–77
9. Guimaraes AR, Siqueira L, Uppal R et al (2016) T2 relaxation time is related to liver fibrosis severity. Quant Imaging Med Surg 6:103–114
10. Koinuma M, Ohashi I, Hanafusa K, Shibuya H (2005) Apparent diffusion coefficient measurements with diffusion-weighted magnetic resonance imaging for evaluation of hepatic fibrosis. J Magn Reson Imaging 22:80–85
11. Yin M, Glaser KJ, Talwalkar JA et al (2016) Hepatic MR elastography: clinical performance in a series of 1,377 consecutive examinations. Radiology 278:114–124
12. Garteiser P, Doblas S, Van Beers BE (2018) Magnetic resonance elastography of liver and spleen: methods and applications. NMR Biomed 31:e3891
13. Nedredal GI, Yin M, McKenzie T et al (2011) Portal hypertension correlates with splenic stiffness as measured with MR elastography. J Magn Reson Imaging 34:79–87
14. Ronot M, Lambert S, Elkrief L et al (2014) Assessment of portal hypertension and high-risk oesophageal varices with liver and spleen three-dimensional multifrequency MR elastography in liver cirrhosis. Eur Radiol 24:1394–1402
15. Lin ZH, Xin YN, Dong QJ et al (2011) Performance of the aspartate aminotransferase-to-platelet ratio index for the staging of hepatitis C-related fibrosis: an updated meta-analysis. Hepatology 53:726–736
16. Wai CT, Greenson JK, Fontana RJ et al (2003) A simple noninvasive index can predict both significant fibrosis and cirrhosis in patients with chronic hepatitis C. Hepatology 38:518–526
17. Kim SY, Seok JY, Han SJ, Koh H (2010) Assessment of liver fibrosis and cirrhosis by aspartate aminotransferase-to-platelet ratio index in children with biliary atresia. J Pediatr Gastroenterol Nutr 51:198–202
18. Chou R, Wasson N (2013) Blood tests to diagnose fibrosis or cirrhosis in patients with chronic hepatitis C virus infection: a systematic review. Ann Intern Med 158:807–820
19. Sterling RK, Lissen E, Clumeck N et al (2006) Development of a simple noninvasive index to predict significant fibrosis in patients with HIV/HCV coinfection. Hepatology 43:1317–1325
20. Messroghli DR, Radjenovic A, Kozerke S et al (2004) Modified Look-Locker inversion recovery (MOLLI) for high-resolution T1 mapping of the heart. Magn Reson Med 52:141–146
21. Megremis SD, Vlachonikolis IG, Tsilimigaki AM (2004) Spleen length in childhood with US: normal values based on age, sex, and somatometric parameters. Radiology 231:129–134
22. Xanthakos SA, Podberesky DJ, Serai SD et al (2014) Use of magnetic resonance elastography to assess hepatic fibrosis in children with chronic liver disease. J Pediatr 164:186–188